Helicobacter pylori Induces Snail Expression Through ROS-Mediated Activation of Erk and Inactivation of GSK-3β in Human Gastric Cancer Cells

Hoang-Kieu-Chi Ngo,[1] Hee Geum Lee,[1] Juan-Yu Piao,[1] Xiancai Zhong,[1] Ha-Na Lee,[1] Hyeong-Jun Han,[1] Wonki Kim,[1] Do-Hee Kim,[1] Young-Nam Cha,[2] Hye-Kyung Na,[3] and Young-Joon Surh[1,4,5]*

[1]*Tumor Microenvironment Global Core Research Center, College of Pharmacy, Seoul National University, Seoul, South Korea*
[2]*Department of Pharmacology, College of Medicine, Inha University, Incheon, South Korea*
[3]*Department of Food and Nutrition, Sungshin Women's University, Seoul, South Korea*
[4]*Department of Molecular Medicine and Biopharmaceutical Sciences, Graduate School of Convergence Science and Technology, Seoul National University, Seoul, South Korea*
[5]*Cancer Research Institute, Seoul National University, Seoul, South Korea*

Helicobacter pylori (*H. pylori*) infection has been known to be implicated in human gastric carcinogenesis. Snail, the zinc-finger transcription factor known as a key inducer of changes in the cell shape and morphogenetic movement, is aberrantly overexpressed and correlates with lymph node metastasis in gastric cancer. In the present study, we investigated whether *H. pylori* could induce Snail activation to provoke these changes. Using a cell scatter assay, we noticed that human gastric cancer AGS cells infected with *H. pylori* underwent morphological changes as well as disruption of cell–cell interaction, which was then reversed by silencing of *Snail* by use of small interfering RNA (siRNA). In addition, infection with *H. pylori* resulted in an increased intracellular level of Snail in gastric cancer cells, which was abrogated in the presence of U0126 and LY294002, inhibitors of MEK/Erk and PI3K/Akt pathways, respectively. Cycloheximide pulse-chase experiments coupled with immunocytochemical analysis revealed that the induction of Snail by *H. pylori* was regulated at multiple levels, including increased transcription of *Snail* mRNA, inhibition of protein degradation, and enhancement of nuclear translocation of Snail. Pre-treatment of AGS cells with *N*-acetylcysteine, a well-known reactive oxygen species (ROS) scavenger, attenuated the *H. pylori*-induced activation of Erk, its binding to *Snail* promoter, inactivation of GSK-3β, and accumulation of Snail. Collectively, these findings suggest that the upregulation of Snail expression induced by *H. pylori* and transformation to a spindle-like shape as a consequence in gastric cancer cells are attributable to ROS-mediated activation of Erk and the inhibition of GSK-3β signaling.

Key words: *Helicobacter pylori*; epithelial mesenchymal transition; Snail; gastric carcinogenesis

INTRODUCTION

Helicobacter pylori (*H. pylori*), a gram-negative bacterium, infects approximately half of the world's population, possibly reaching up to 70% in developing countries and 20–30% in industrialized nations [1]. *H. pylori* infection has been speculated as a principal risk factor causing gastritis and gastric cancer. Although most *H. pylori*-infected individuals only experience chronic gastritis, a small subset of chronically infected population develops gastric adenocarcinoma [2,3]. *H. pylori* infection triggers a sequence of alterations in the gastric mucosa, starting with superficial gastritis which can progress to chronic gastritis, atrophic gastritis, intestinal metaplasia, dysplasia and finally, gastric carcinoma [4]. Results from recent studies suggest that chronic infection with *H. pylori* is associated with an increase in epithelial-mesenchymal transition (EMT) which is implicated in gastric cancer progression and metastasis [5,6]. However, the mechanisms underlying *H. pylori*-induced EMT remain largely unclarified. During EMT, epithelial cells acquire fibroblast-like properties with reduced intercellular adhesion and increased motility, which facilitates tumor invasion and metastasis. Initially, epithelial cells with tight intercellular adhesion lined by basement membrane

Abbreviations: *H. pylori*, *Helicobacter pylori*; ROS, reactive oxygen species; WT, wild type; EMT, epithelial-mesenchymal transition; Erk, extracellular signal-related kinase; MEK or also known as MAP2K, mitogen-activated protein kinase kinase; PI3K, phosphoinositide-3-kinase; GSK-3β, glycogen synthase kinase-3β; SDS–PAGE, sodium dodecyl sulphate-polyacrylamide gel electrophoresis; siRNA, small interfering RNA; NAC, *N*-acetyl-L-cysteine; DCF-DA, 2′,7′-dichlorofluorescein diacetate; CHX, cycloheximide; PI, propidium iodide; DAPI, 4′,6-diamidino-2-phenylindole.

Conflict of interest: All authors declare no conflict of interest.

Grant sponsor: Global Core Research Center; Grant number: 2011-0030001; Grant sponsor: National Research Foundation

*Correspondence to: Tumor Microenvironment Global Core Research Center, College of Pharmacy, Seoul National University, 1 Gwanak-ro, Gwanak-gu, Seoul 151-742, South Korea.

Received 7 May 2015; Revised 3 January 2016; Accepted 8 January 2016

DOI 10.1002/mc.22464

Published online in Wiley Online Library (wileyonlinelibrary.com).

can grow abnormally and proliferate locally to give rise to the formation of adenoma. Further epigenetic and genetic alterations result in carcinoma in situ. When in situ carcinoma cells undergo EMT, they can intravasate into lymphatic or blood vessels, and migrate to distant organs as a consequence of basement membrane fragmentation. The transcription factor Snail has been considered as one of the key regulators of EMT [7,8]. In addition, overexpression of Snail was found to be associated with lymph node metastasis and poor prognosis in patients with gastric cancer [9]. In the present study, we found that *H. pylori* infection could induce EMT through overproduction of reactive oxygens species and subsequent Snail upregulation in human gastric cancer cells.

MATERIALS AND METHODS

Materials

RPMI-1640 medium, DMEM medium, fetal bovine serum, penicillin, and streptomycin were products of GIBCO BRL (Grand Island, NY). Sheep blood agar, Gaspak™ and anaerobic jars were provided by BD Biosciences (Sparks, MD). U0126 and LY294002 were purchased from TOCRIS (Ellisville, MO). Carbobenzoxy-leucyl-leucyl-leucinal (MG132) was a product from Enzo Life Science (Farmingdale, NY). Phenylmethylsulfonyl fluoride (PMSF), cycloheximide (CHX), dithiothreitol (DTT), *N*-acetylcysteine (NAC), and primary antibody against actin were products of Sigma–Aldrich Co. (St. Louis, MO). Primary antibodies for Snail, GAPDH, and lamin B were from Santa Cruz Biotechnology (Santa Cruz, CA). CagA primary antibody was provided by AUSTRAL Biologicals (San Ramon, CA). Antibodies against hemagglutinin (HA), total extracellular signal-regulated kinase (Erk) 1, phospho-Erk 1/2, Akt, phospho-Akt, glycogen synthase kinase-3β (GSK-3β), and phospho-GSK-3β were purchased from Cell Signaling Technology (Beverly, MA). Primary antibody for α-Tubulin was a product from Biogenex (Fremont, CA). Horseradish peroxidise-conjugated secondary antibodies were obtained from Pierce Biotechnology (Rockford, IL). The antibody against occludin, Alexa 488 conjugated-IgG, Alexa 546 conjugated-IgG, TRIzol®, 2′,7′-dichlorofluorescein diacetate (DCF-DA), propidium iodide (PI), 4′,6-diamidino-2-phenylindole (DAPI), SYBR®, Lipofectamine® 2000, Lipofectamine® RNAiMAX, and Steath™ RNAi negative control duplexes were provided by Invitrogen (Carlsbad, CA). Human Snail-specific siRNA duplex (5′-GCGAGCUGCAGGACUCUAA-3′) was purchased from Genolution Pharmaceuticals, Inc. (Seoul, South Korea). Polyvinylidene difluoride (PVDF) membranes were supplied from Gelman laboratory (Ann Arbor, MI). Protease inhibitor cocktail tablets were provided from Boehringer Mannheimm (Mannheimm, Germany). A protein assay dye (Bradford) reagent was supplied by Bio-Rad Laboratories (Hercules, CA). The bicinchonic acid (BCA) protein assay reagent was obtained from Pierce Biotechnology (Rockford, IL).

Cell Culture

The human gastric cancer cell lines (AGS, MKN-1 and MKN-45) and the human colon cancer cell line (HCT116) were obtained from the American Type Culture Collection (ATCC, Rockville, MD). AGS, MKN-1 and MKN-45 cells were cultured in RPMI-1640 and HCT116 cells were maintained in DMEM medium supplemented with 10% v/v FBS and 100 units/mL penicillin and 100 μg/mL streptomycin at 37°C in an incubator with humidified atmosphere of 5% CO_2.

Plasmid

Mammalian expression vector for CagA (pSP65SRα WT CagA-HA) was generously provided by Prof. M. Hatakeyama (The University of Tokyo, Japan) and Prof. Yong Chan Lee (Yonsei University College of Medicine, Seoul, South Korea). AGS cells were transfected with wild-type (WT) CagA-HA vector using the transfection reagent Lipofectamine 2000 for 24 h following the manufacturer's instructions and then harvested for subsequent experiments.

H. pylori Strain and Growth Condition

Isolates of *H. pylori* (ATCC 43504, *cag* PAI, and *vac* A positive strain) obtained from ATCC were grown on 5% sheep blood agar plates with antibiotic supplements (Dents supplement) (Oxoid, Basingstoke, UK) at 37°C under microaerophilic conditions generated by CampyPack plus in an atmosphere of 5% O_2, 10% CO_2, and 85% N_2 for 48 h.

H. pylori Infection of Cultured Gastric Cancer Cells

The cells were seeded in tissue culture plates for 24 h. For the infection, *H. pylori* harvested in Brucella broth (Difco BD; Sparks, MD) containing 10% FBS were added to the host cells at a multiplicity of infection (MOI) of 100. U0126 (20 μM), LY294002 (20 μM), MG132 (20 μM), and NAC (20 mM) were added to the cells in culture 1 h before the *H. pylori* infection.

Scattering Assay

Subconfluent cultures of AGS cells were infected with *H. pylori* for 10 h in the presence or absence of Snail siRNA. Morphologic changes that occur in *H. pylori* infected cell colonies were assessed by light microscopy. Scattered colony formation was verified by dissociation of cell–cell adhesion and the acquisition of a migratory phenotype with a typical change to spindle-shaped morphology.

Western Blot Analysis

After the *H. pylori* infection, cells were lysed in 1 × lysis buffer [100 mM Tris-HCl (pH 7.5), 150 mM NaCl, 5 mM EDTA (pH 8.0), 1% Triton X-100, 5 mM DTT, 10% glycerol, protease inhibitor cocktail tablets,

and 1% PMSF]. The protein concentration was measured by the Bradford method using the Bio-Rad protein assay dye. In some experiments, cytosolic and nuclear proteins were prepared according to the procedure described elsewhere [10]. The solubilized proteins were subjected to sodium dodecyl sulphate (SDS)-polyacrylamide gel electrophoresis (PAGE). Thereafter, the separated proteins were transferred to PVDF membrane. Membranes were probed separately with various antibodies, and blots were visualized according to the procedure described previously [10].

Reverse Transcription Polymerase Chain Reaction (RT-PCR)

Total RNA isolated from variously treated AGS cells using TRIzol® was used for the complementary DNA (cDNA) synthesis. RT-PCR was performed following a standard procedure. The primer pairs for PCR of the expected products were as follows (forward and reverse, respectively): *Snail*, 5′-CCT GCT GGC AGC CAT CCC AC-3′ and 5′-GGC AGC GTG TGG CTT CGG AT-3′ and *GAPDH*, 5′-ACC CAG AAG ACT GTG GAT GG-3′ and 5′-TCT AGA CGG CAG GTC AGG TC-3′. Amplified products were resolved by 1.5% agarose gel electrophoresis, stained with SYBR® and visualized with the imagequant™ LAS 4000.

Quantitative Real-Time Polymerase Chain Reaction (qPCR)

qPCR was performed using RealHelix™ qPCR kit (Nanohelix; Daejeon, South Korea) with Applied Biosystem 7500 Fast Real-Time PCR System (Applied Biosystem; Grand Island, NY). The relative RNA expression levels were determined according to the comparative threshold cycle (Ct value) method with *GAPDH* as an internal control. The primers used in qPCR analysis were as follows: *Snail*, 5′-TGC TCA TCT GGG ACT CTG TC-3′ and 5′-CTC ATC TGA CAG GGA GGT CA-3′ and *GAPDH*, 5′-AAT CCC ATC ACC ATC TTC CA-3′ and 5′-TGG ACT CCA CGA CGT ACT CA-3′.

Chromatin Immunoprecipitation (ChIP) Assay

The ChIP assay was performed using a commercially available kit provided by Milipore (17-371/EZ-ChIP™, Merck KGaA, Darmstadt, Germany) following manufacturer's directions. Briefly, after treated with *H. pylori* in the presence or absence of NAC for 5 h, AGS cells were cross-linked with 1% formaldehyde at room temperature and quenched in glycine. The protein-chromatin complexes in cell lysates were first immunoprecipitated with anti-Erk antibody, followed by incubation with Protein G-conjugated agarose beads. The complexes were washed extensively to eliminate non-specific bindings and incubated at 65°C to dissociate protein-DNA crosslinks. DNA was purified and subjected to qPCR using the following primers: F: 5′-GTG TCC CTT TCC TCG CTT C-3′ and R: 5′-GGA CAC CTG ACC TTC CGA-3′, which allow the amplification of *Snail* promoter region (-869/+59 *Snail* promoter). One percent of chromatin before immunoprecipitation was included as the input control.

Snail-siRNA Transient Transfection

AGS cells were transfected with Snail-siRNA or control siRNA using the transfection reagent Lipofectamine RNAiMAX for 24 h following the manufacturer's instructions. Transfected cells were then treated with *H. pylori* for the indicated times and then harvested for the next experiments.

Immunocytochemical Analysis

Immunocytochemistry was conducted with the AGS cells transfected with CagA-HA vector or infected with *H. pylori*. After fixation with 4% paraformaldehyde for 20 min at room temperature, cells were permeabilized with 0.2% Triton X-100 and then blocked with 5% bovine serum albumin in PBST (PBS containing 0.1% Tween-20) for 2 h at room temperature. Permeabilized cells were then stained with the primary antibodies overnight at 4°C, followed by incubation with Alexa 488 and 546 secondary antibodies for 1 h at room temperature. Nuclear-staining was performed with PI or DAPI for 10 min at room temperature. Images were assessed under a confocal microscopy (LSM 700, Zeiss, Oberkochen, Germany).

Measurement of ROS Accumulation

Accumulation of ROS in the AGS cells infected with *H. pylori* was monitored using the ROS-derived fluorescence-generating probe DCF-DA. Treated cells were rinsed with PBS and loaded with 10 μM DCF-DA. After 30 min of incubation at 37°C, cells were examined under a fluorescent microscopy (Leica, Wetzlar, Germany) set at 488 nm for excitation and 530 nm for emission.

Statistical Analysis

Data obtained from at least three independent experiments were expressed as the mean ± s.e.m. The statistical significance of differences between two groups was evaluated using two-tailed Student's *t*-test. Analysis was performed using Graphpad Prism (Version 6). Statistical significance was accepted at $P < 0.05$, unless otherwise indicated.

RESULTS

H. pylori Infection Disrupts Cell–Cell Interaction and Upregulates Snail Expression in Gastric Cancer Cells

The morphological changes of AGS cells treated with *H. pylori* were assessed by phase contrast microscopy. Upon exposure to *H. pylori*, AGS cell colonies became dispersed, displaying a spindle-like appearance. Moreover, the number of scattered colonies, reflecting enhanced cell motility and invasiveness, was increased compared with that of the non-infected controls (Figure 1A). Occludin

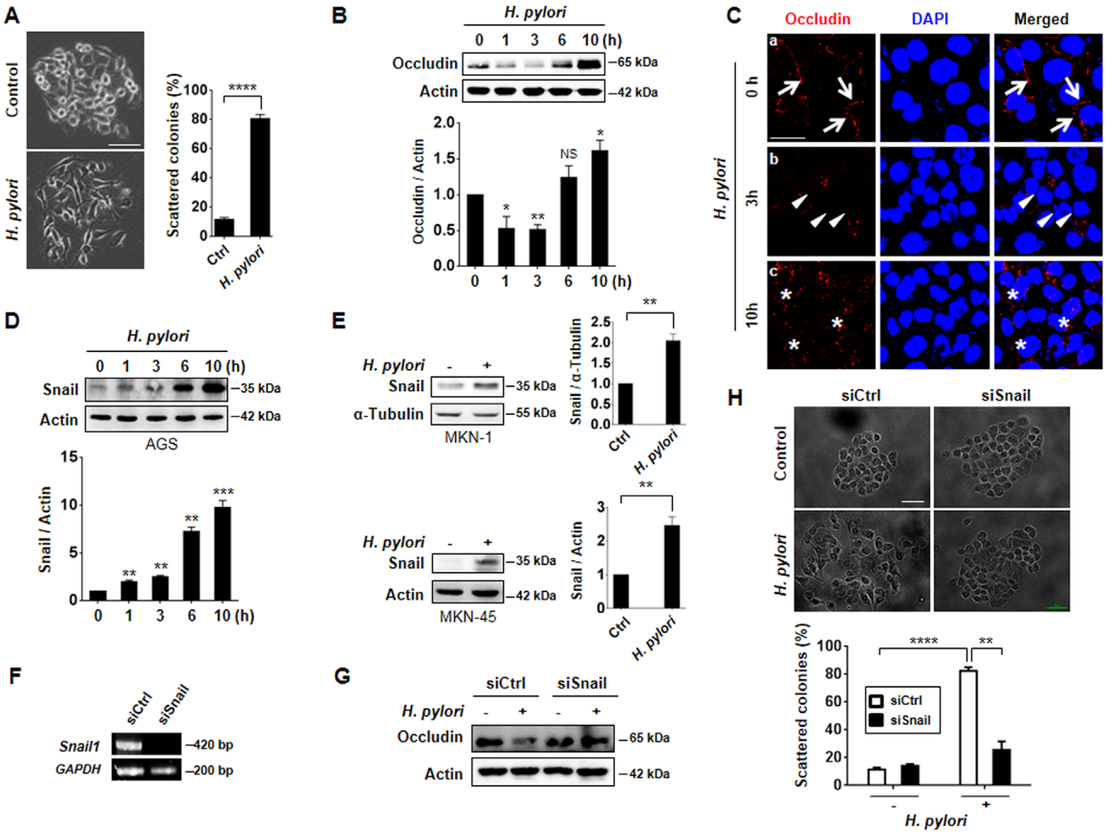

Figure 1. Disrupted cell–cell interaction and upregulated Snail expression in *H. pylori*-treated human gastric cancer cells. (A) AGS cells co-incubated with *H. pylori* for 10 h were subjected to the cell scatter assay. Representative images show a spindle-like shape as well as destruction of direct interaction between cells. The number of scattered colonies was scored. (B–C) AGS cells were treated with *H. pylori* for the indicated times, followed by immunoblotting (B) or immunocytochemical analysis (C) with occludin antibody. Actin was included to ensure equal protein loading. Immunoblots were quantified by densitometry. DAPI was co-stained with occludin primary antibody to show contrast. (D) AGS cells were treated with *H. pylori* for the indicated times, followed by immunoblotting with Snail antibody. Immunoblots were quantified by densitometry. (E) MKN-1 and MKN-45 cells were treated with *H. pylori* for 6 h, followed by immunoblotting with Snail antibody. (F) AGS cells were transfected with either control siRNA or Snail siRNA for 24 h. Total RNA was then extracted and analyzed by RT-PCR with *Snail* sequence-specific primers, verifying complete silencing of *Snail*. *GAPDH* was used as an internal control. (G–H) Control siRNA or Snail siRNA transfected AGS cells were treated with *H. pylori* for 3 h (G) or 10 h (H). (G) Whole-cell lysastes were prepared and subjected to Western blot analysis with occludin primary antibody. (H) Phase contrast microscopy reveals that the *H. pylori*-caused hummingbird phenotype and intercellular separation are abrogated by siRNA knock down of *Snail*. All results are presented as mean ± s.e.m; $^{*}P < 0.05$, $^{**}P < 0.01$, $^{***}P < 0.001$, $^{****}P < 0.0001$, NS: non-significant. Scale bar: 50 μm (A, C, H). Arrow: occludin at cell margin, triangle: disruption of occludin at cell margin, asterisk: occludin in cytoplasm.

is an integral membrane protein localized at tight junctions, which is responsible for establishing and maintaining epithelial cell polarity [11]. The levels of total occludin (Figure 1B) and occludin at tight junctions (Figure 1C-a and b) were markedly diminished by *H. pylori* infection for 3 h, indicative of EMT induction. In contrast, *H. pylori* infection for 10 h induced expression of occludin, but this was mainly localized in cytoplasm rather than at tight junctions (Figure 1C-c). Activation of the transcription factor Snail has been known to play a key role in the induction of EMT, which accompanies distinct morphological changes, acquisition of migratory properties and concomitant repression of occludin expression [11,12]. In the *H. pylori*-treated AGS cells, a time-dependent increase in Snail expression was observed (Figure 1D). The induction of Snail expression by *H. pylori* was also noticed in other human gastric cancer cell lines including MKN1 and MKN45 (Figure 1E). To further verify the role of Snail in the *H. pylori*-mediated induction of EMT in AGS cells, we utilized siRNA specifically targeting *Snail*. The effectiveness of Snail siRNA to knock down the *Snail* expression was confirmed by RT-PCR (Figure 1F). The suppression of occludin caused by *H. pylori* after 3 h of infection was abrogated in the presence of Snail siRNA (Figure 1G). In addition, as illustrated in Figure 1H, the transition to the hummingbird phenotype as well as intercellular separation of AGS cell colonies caused by *H. pylori* infection was attenuated by silencing of *Snail*.

The ROS Scavenger NAC Attenuates *H. pylori*-Induced Snail Expression

The CagA bacterial oncoprotein is speculated to play a critical role in gastric carcinogenesis by *H. pylori*. Once delivered into epithelial cells, CagA causes loss of cell polarity and elongated cell morphology [13]. We noticed that CagA-transfected AGS cells exhibited the hummingbird phenotype (Figure 2A) and slightly enhanced Snail expression (Figure 2B), in agreement with results from other studies [14,15]. However, AGS cells infected with CagA-positive *H. pylori*, even though much smaller amount of CagA was accumulated, displayed a much higher expression level of Snail compared to that in CagA-transfected cells, (Figure 2C), indicative of the involvement of other factors derived from *H. pylori* in induction of Snail. Therefore, the capability of *H. pylori* to upregulate Snail to a greater extent than exogenous CagA would be largely attributable to elements other than CagA derived from this bacterium.

Accumulation of moderate amounts of intracellular ROS often alters gene expression [16,17] and stimulates cell invasiveness [18,19]. *H. pylori* infection has been reported to enhance the generation of intracellular ROS in gastric epithelial cells [20,21]. Thus, we speculated that *H. pylori*-induced upregulation of Snail expression might be mediated by ROS. We initially measured the accumulation of ROS after *H. pylori* exposure using the oxidant-sensitive fluorescent probe DCF-DA. The enhancement of ROS production by *H. pylori* was detected in AGS cells (Figure 2D, upper right). The pretreatment of AGS cells with the ROS scavenger NAC abolished not only the ROS accumulation (Figure 2D, lower right) but also the upregulation of Snail expression (Figure 2E) in *H. pylori*-treated cells. These findings suggest that the

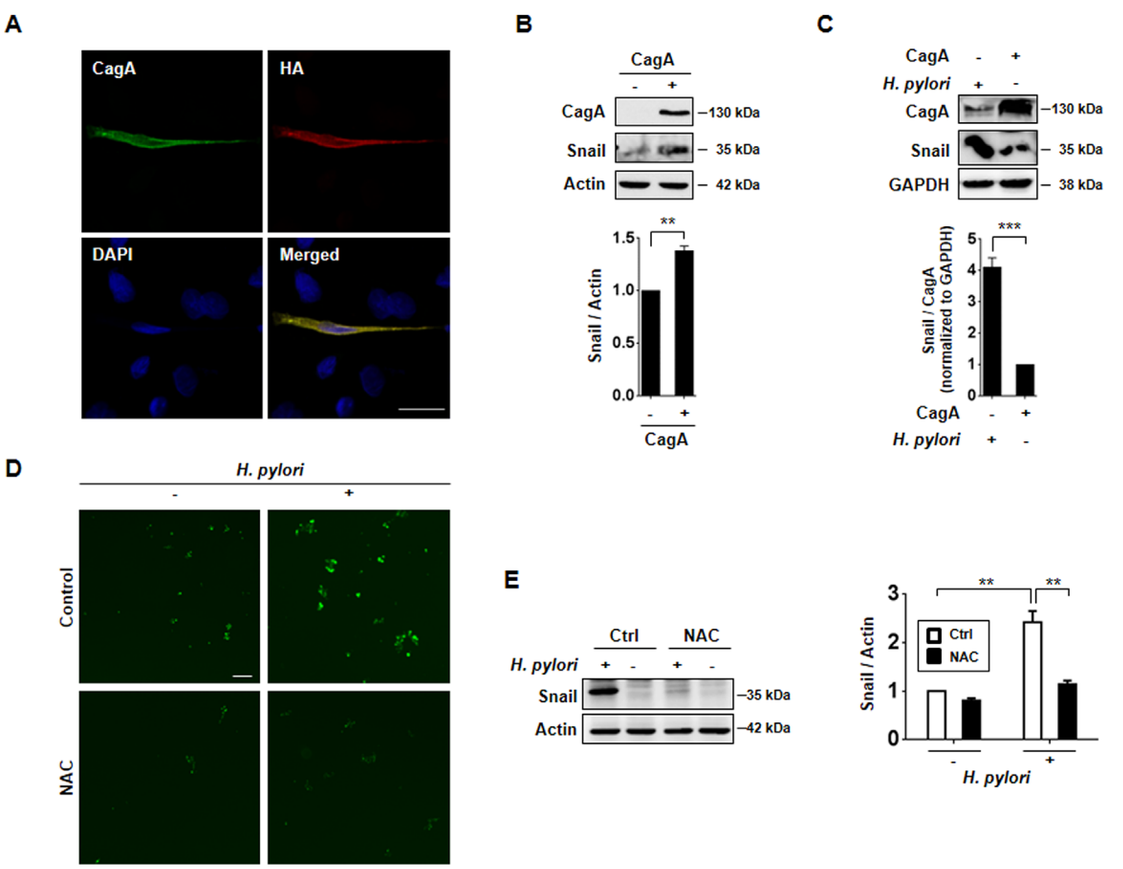

Figure 2. Possible involvement of ROS in *H. pylori*-induced Snail expression. (A) AGS cells were transfected with CagA-HA vector for 24 h, followed by immunocytochemical analysis with CagA and HA antibodies. DAPI was counter stained. (B–C) AGS cells were transfected with CagA-HA vector or infected with *H. pylori*. Whole-cell lysastes were prepared and subjected to Western blot analysis with Snail antibody. Actin and GAPDH were used as equal loading controls (D–E) AGS cells were treated with NAC for 1 h prior to exposure to *H. pylori* for 30 min (D) or 3 h (E). (D) Cells were then washed and incubated with DCF-DA, followed by fluorescent microscopy. (E) Whole-cell lysastes were prepared and subjected to Western blot analysis with Snail antibody. Data represent mean ± s.e.m of three independent assays. $^{**}P < 0.01$, $^{***}P < 0.001$. Scale bar: 20 μm (A), 200 μm (C).

H. pylori-induced Snail expression in AGS cells is mediated, at least in part, by ROS.

Erk Upregulates *H. pylori*-Induced Snail Expression

It has been shown that production of ROS results in activation of the Erk cascade in response to diverse stimuli [22]. Activation of the Erk pathway not only controls cell proliferation and survival but also cancer cell motility, invasion, and metastasis [23,24]. Therefore, we investigated whether the activation of Erk is involved in the upregulation of Snail expression in *H. pylori*-infected cells. *H. pylori* infection caused a transient increase in the phosphorylation of Erk (Figure 3A). To confirm the role of Erk in the upregulation of Snail expression induced by *H. pylori* infection, U0126 (an inhibitor of MEK, upstream of Erk) was utilized. The pharmacological inhibition of MEK-Erk signaling abolished the phosphorylation of Erk induced by *H. pylori* infection (Figure 3B). In addition, pretreatment of AGS cells with U0126 blunted *H. pylori*-induced Snail expression at both protein (Figure 3C) and mRNA (Figure 3D) levels. We also noticed that preincubation of AGS cells with NAC abolished the activation of Erk caused by the *H. pylori* infection (Figure 3E). Several lines of evidence indicate that Erk binds directly to the *Snail* promoter (−869/+59), driving transcription of *Snail* [25,26]. Accordingly, we carried out ChIP-qPCR analysis using Erk antibody and specific primers harbouring a sequence from −869 to +59 of the *Snail* promoter in AGS cells treated with *H. pylori* in the presence or absence of NAC. The result of this experiment revealed that NAC was able to suppress the binding of Erk to the *Snail* promoter (Figure 3F). These data suggest that *H. pylori*-induced upregulation of Snail expression through Erk activation is likely to be mediated by ROS.

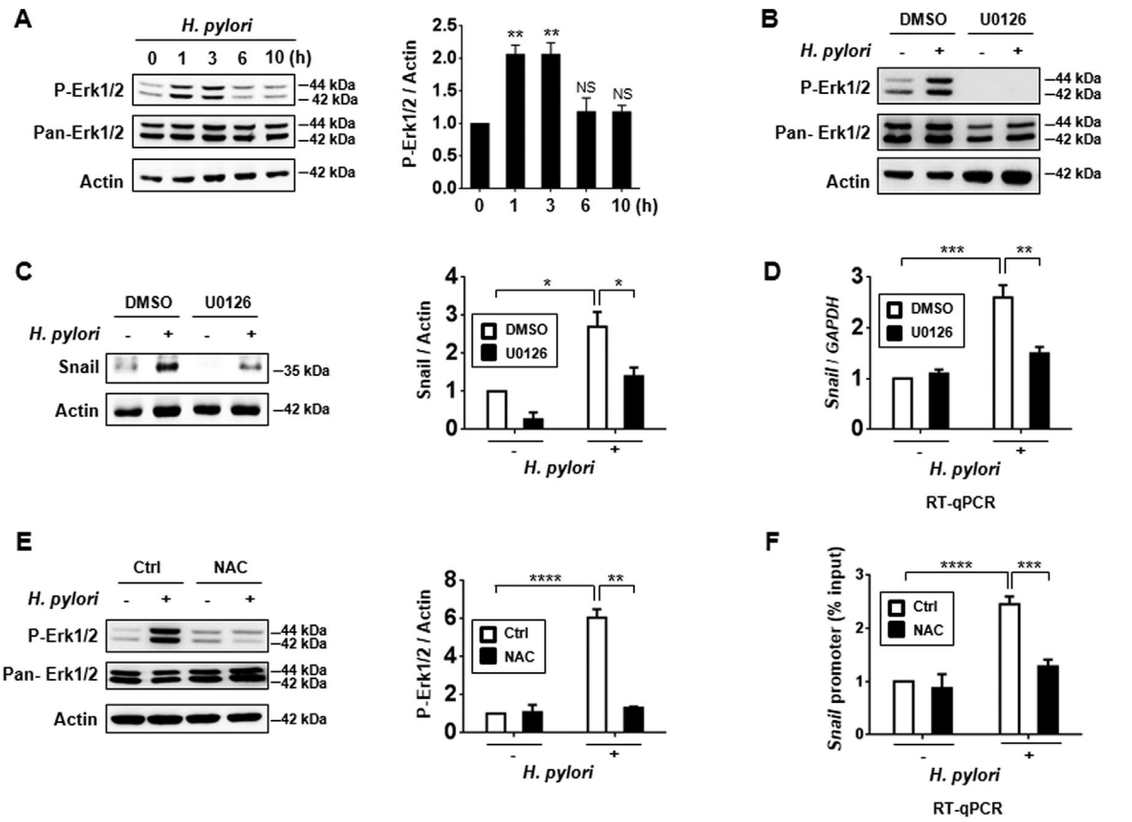

Figure 3. Role of Erk in *H. pylori*-induced Snail expression. (A) Whole-cell lysates from AGS cells treated with *H. pylori* were subjectd to Western blot analysis. Densitometric quantification of P-Erk1/2 is shown. (B–D) Cells were pretreated with 20 μM of U0126, an MEK inhibitor, for 1 h prior to incubation with *H. pylori* for additional 3 h. (B) Levels of P-Erk1/2 were determined by Western blot analysis, showing complete inhibition of Erk1/2 phosphorylation by U0126. (C) Abrogation of *H. pylori*-induced Snail expression by U0126. Densitometric quantification of Snail is shown. (D) Total RNA was prepared for RT-qPCR with primers specific for *Snail*. Inhibition of *H. pylori*-induced *Snail* mRNA expression by U0126. (E) AGS cells were treated with NAC for 1 h prior to exposure to *H. pylori* for 3 h. Phosphorylation of Erk1/2 triggered by *H. pylori* was almost completely abolished by NAC treatment. (F) AGS cells were treated with *H. pylori* in the presence or absence of NAC. Cell lysates were then prepared and subjected to ChIP with Erk antibody. ChIP-enriched DNA was amplified and analyzed by qPCR using primers specific for −869/+59 *Snail* promoter region. One percent of the chromatin before immunoprecipitation served as input. Data represent mean ± s.e.m of three independent assays. $^{*}P < 0.05$, $^{**}P < 0.01$, $^{***}P < 0.001$, $^{****}P < 0.0001$, NS: non-significant.

The PI3K/Akt/GSK-3β Axis Is Involved in the Induction of Snail Expression by *H. pylori*

GSK-3β, a kinase located in the downstream of the PI3K/Akt pathway, has been known to act as an endogenous inhibitor of Snail by stimulating proteasomal degradation of this transcription factor [27,28]. Notably, GSK-3β became inactivated through phosphorylation at Ser9 upon *H. pylori* infection, which appears to be attributable to activation of the PI3K/Akt signaling (Figure 4A). To confirm that suppression of GSK-3β activity by PI3K/Akt could account for the upregulation of Snail by *H. pylori*, we treated AGS cells with LY294002, a PI3K inhibitor, and then examined the *H. pylori*-induced expression of P-GSK-3β and Snail as well as P-Akt. We found that pharmacologic inhibition of the PI3K-Akt axis abolished the *H. pylori*-induced phosphorylation of GSK-3β (Figure 4B). In addition, the pretreatment with LY294002 also attenuated the expression of Snail induced by *H. pylori* infection (Figure 4C) without affecting the *Snail* mRNA expression (Figure 4D). Notably, the *H. pylori*-derived inactivation of GSK-3β was suppressed by preincubation of AGS cells with NAC (Figure 4E). According to previous studies, Erk could act upstream of GSK-3β [29,30]. However, we did not see any substantial changes in phosphorylation of GSK-3β by *H. pylori* when the MEK-Erk signaling was blocked by U0126 (Figure 4F).

H. pylori Increases Protein Stability and Nuclear Translocation of Snail

Snail has been discovered as a highly unstable protein with a half-life of approximately 25 min [31]. In agreement with this notion, Snail protein is barely detectable in the *H. pylori*-untreated AGS cells. Thus, we conducted a chase experiment by using CHX, a protein synthesis inhibitor, to more precisely assess the stability of Snail protein in the presence of

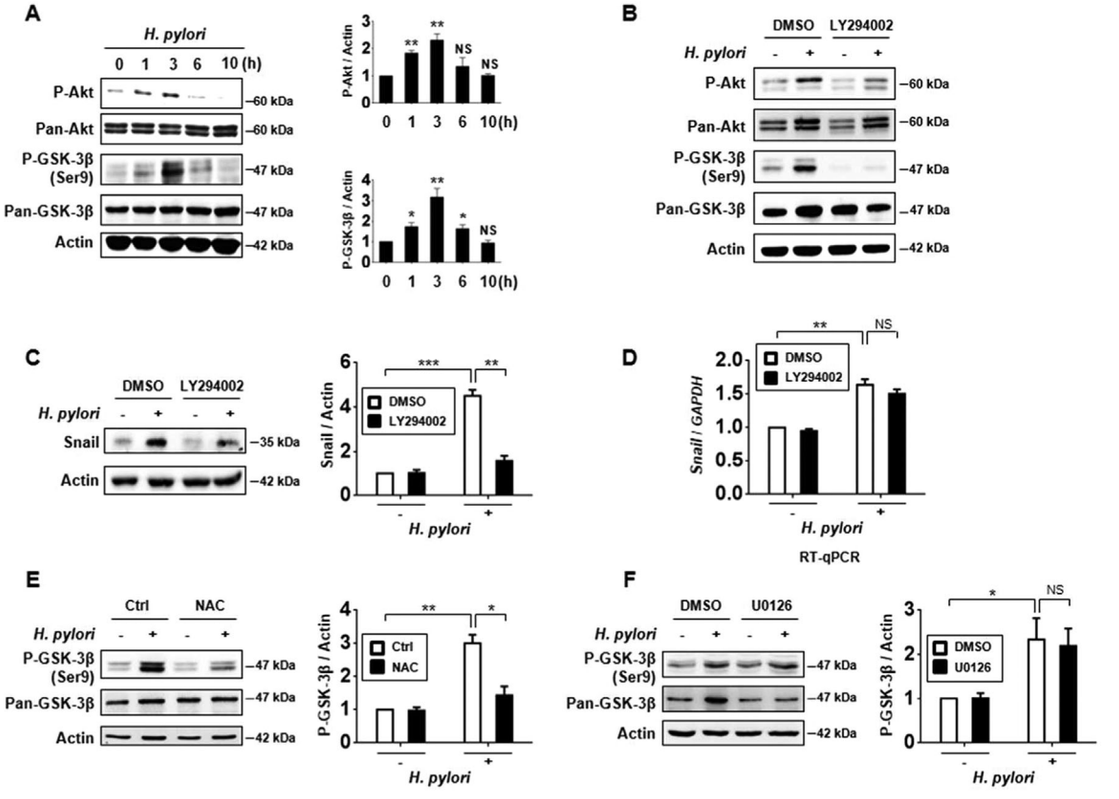

Figure 4. Involvement of the PI3K/Akt/GSK-3β axis in the induction of Snail expression by *H. pylori*. (A) AGS cells were treated with *H. pylori* and whole-cell lysates were prepared for Western blot analysis of P-Akt and P-GSK-3β. Densitometric quantification of P-Akt and P-GSK-3β is shown. (B–D) Cells were pre-incubated with 20 μM of LY294002, a PI3K inhibitor, for 1 h prior to co-incubation with *H. pylori* for additional 3 h. (B) Complete inhibition of phosphorylation of Akt as well as GSK3-β by LY294002. (C) Inhibitory effects of LY294002 on *H. pylori*-induced Snail expression. Intensity of Snail bands was quantified. (D) Total RNA was prepared for RT-qPCR with specific primers for *Snail*. LY294002 failed to inhibit *H. pylori*-induced *Snail* mRNA expression. The histogram represents quantification of *Snail* mRNA levels. (E) AGS cells were treated with NAC for 1 h prior to exposure to *H. pylori* for 3 h. Phosphorylation of GSK-3β triggered by *H. pylori* was abolished by NAC treatment. (F) AGS cells were treated with U0126 (20 μM) for 1 h prior to *H. pylori* exposure for additional 3 h. Western blotting analysis was performed, showing no effect of U0126 on *H. pylori*-induced phosphorylation of GSK-3β. Data represent mean ± s.e.m of three independent assays. $^{*}P < 0.05$, $^{**}P < 0.01$, $^{***}P < 0.001$, NS: non-significant.

H. pylori. Initially, AGS cells were treated with *H. pylori* for 6 h to induce Snail expression and then exposed to DMSO or CHX. As shown in Figure 5A and B, CHX treatment did not alter the *H. pylori*-induced Snail protein expression profile.

The transcriptional activity of Snail could be affected by its subcellular localization. When localized in cytoplasm, Snail is phosphorylated and subsequently targeted for proteasomal degradation [32]. In the presence of the proteasome inhibitor MG132, Snail is maintained in a phosphorylated and ubiquitinated form. As a result, the migration of Snail on SDS-PAGE gel was found to be delayed [33]. However, Snail from *H. pylori* infected cells moved faster than that from MG132 treated ones (Figure 5C), suggesting the existence of either a non-phosphorylated or a de-ubiquitinated/an unubiquitinated form of Snail that is less prone to degradation by the ubiquitin-proteasome system.

We also noticed a prominent nuclear accumulation of Snail following *H. pylori* infection (Figure 5D). The increased nuclear localization of Snail was further verified by Western blot analysis (Figure 5E).

DISCUSSION

Expression of the transcription factor Snail is a critical determinant in the manifestation of a mesenchymal phenotype characterized by the spindle-like shape and migratory properties that contribute to acquisition of invasiveness of epithelial cells in the tumor microenvironment [26]. In this study, we found that human gastric adenocarcinoma AGS cells transfected with *H. pylori* exhibited upregulated Snail expression with concomitant manifestation of the hummingbird phenotype as well as intercellular separation and increased cell motility.

Our study provides an insight into the mechanism underlying regulation of Snail by *H. pylori* infection. We found that *H. pylori* activated signal transduction mediated by both Erk and PI3K/Akt, which might contribute to an upregulation of Snail expression in *H. pylori*-infected AGS cells. In another study, it was shown that a blockage of the MEK/Erk pathway effectively inhibited the PI3K/Akt/GSK-3β signaling [34]. However, we did not observe any influence of an MEK inhibitor on the phosphorylation of the

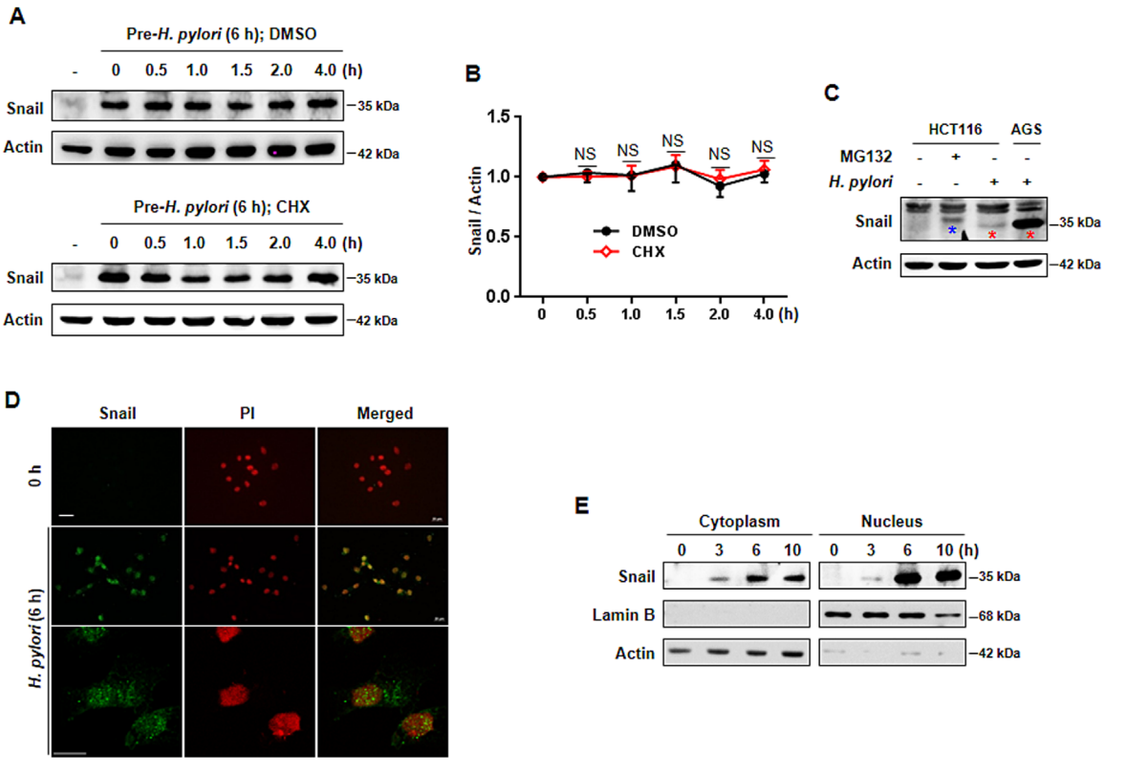

Figure 5. Increased protein stability and nuclear translocation of Snail in cells treated with *H. pylori*. (A–B) AGS cells were pretreated with *H. pylori* for 6 h before exposure to DMSO or CHX (10 μM), and Snail expression was measured. All data are representative of three independent assays. (C) HCT116 cells were treated with MG132 (20 μM), a proteasome inhibitor or *H. pylori* for 6 h. AGS cells were incubated with *H. pylori* alone for 6 h. Whole-cell lysates were subjected to Western blot analysis with Snail-specific antibody. Snail in *H. Pylori*-treated cells migrated faster on SDS-PAGE gel than that in MG132 treated cells. (D) Nuclear accumulation of Snail in AGS cells upon *H. pylori* infection for 6 h was observed by fluorescent microscopy after immunofluorescent staining. Scale bar: 20 μm (top), 10 μm (bottom). (E) Nuclear translocation of Snail was verified by immunoblot analysis. Actin and lamin B were included as loading controls for cytosolic and nuclear fractions, respectively. Data are representative of three independent assays. NS: non-significant.

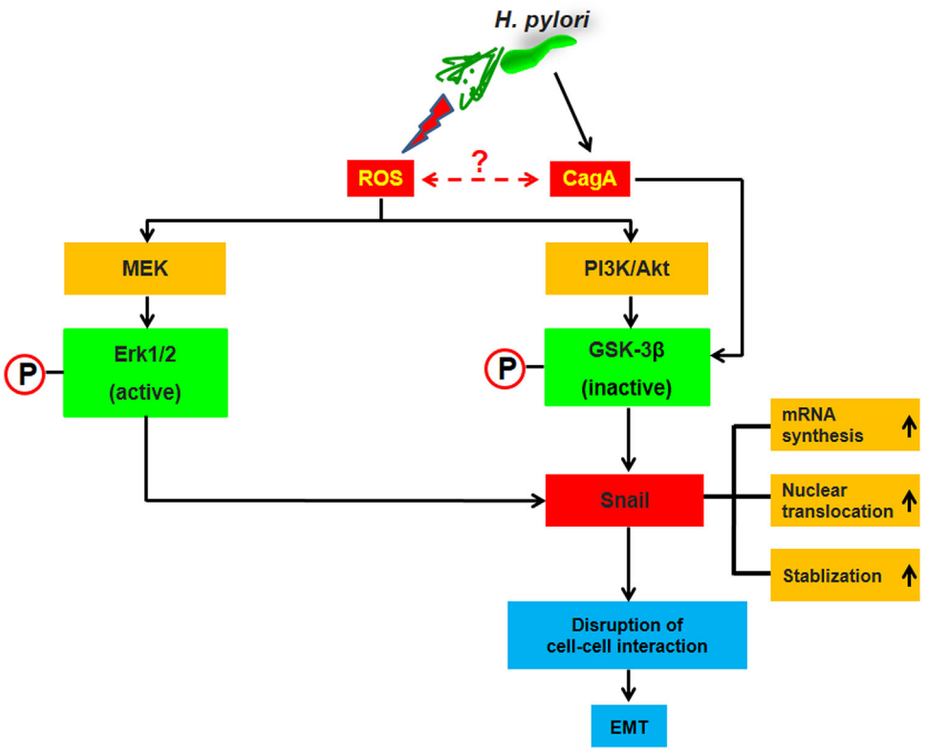

Figure 6. A proposed mechanism underlying *H. pylori* induced Snail accumulation in AGS cells through ROS-mediated activation of Erk and inactivation of GSK-3β. ROS generated as a consequence of *H. pylori* infection activates Erk1/2 through MEK-mediated phosphorylation. The phosphorylated Erk may bind directly to the *Snail* promoter (−869/+59), driving transcription of *Snail* [25,26]. Alternatively, ROS can activate PI3K-Akt signlaing, which in turn phosphorylates and catalytically inactivates GSK-3β. GSK-3β binds to and phosphorylates Snail, resulting in the degradation of Snail. However, inhibitory phosphorylation of GSK3β by Akt will enhance the nuclear accumulation as well as the stability of Snail. The *H. pylori*-derived virulence factor CagA can also promote Snail upregulation and EMT through suppression of GSK-3β activity [15]. Thus, ROS and CagA are speculated to mediate *H. pylori*-induced Snail upregulation and EMT, independently of each other or coordinately.

GSK-3β in *H. pylori*–infected AGS cells. Thus, Erk and GSK-3β might act independently of each other to mediate *H. pylori*-induced Snail expression in AGS cells. Once phosphorylated by *H. pylori*, Erk is likely to regulate expression of Snail at a transcriptional level through direct binding to *Snail* promoter region comprising −869/+59 with respect to translation start. By contrast, GSK-3β appears to mediate expression of Snail at a translational, but not a transcriptional level. It has been reported that Snail activity is regulated by its subcellular localization. When present in the cytoplasm, Snail is phosphorylated by upstream signaling kinases and then degraded via the ubiquitin-proteasome pathway [35–37]. Notably, GSK-3β was shown to bind and phosphorylate Snail at two consensus motifs, thereby differentially modulating the function of this transcription factor. Phosphorylation of the second motif causes Snail to export to the cytoplasm from the nucleus, whereas phosphorylation of the first motif regulates its β-Trcp-mediated ubiquitination, resulting in a reduced stability of Snail with a half-life of approximately 25 min [31]. In our current study, we also noticed that phosphorylation of GSK-3β by *H. pylori*, which keeps this kinase in an inactivated state, elevated the protein level of Snail without affecting expression of its mRNA transcript, corroborating the role of GSK-3β in modulating the stability of Snail protein.

While our manuscript was being in preparation, Lee et al. have reported that *H. pylori*-derived virulence factor CagA promotes Snail-mediated EMT through suppression of GSK-3β activity [15]. According to this study, CagA was proposed to bind to GSK-3β and consequently inhibit its kinase activity in a manner similar to canonical Wnt activation [15]. CagA is likely to be one of the bona fide Snail inducers as demonstrated by use of a CagA mutant type of *H. pylori* [15]. However, we noticed that *H. pylori* appears to be far more effective than CagA in terms of inducing Snail expression.

A salient feature of our present study is that ROS overproduced in response to *H. pylori* infection, probably due to mitochondria dysfunction [38], contributes to the increased expression of Snail by this bacterium. Our findings clearly reveal that *H. pylori* infection of AGS cells elevates Snail expression

via ROS-mediated activation of Erk and inactivation of GSK3β. ROS and CagA either independently of each other or coordinately mediate *H. pylori*-induced Snail expression.

We found that *H. pylori*-induced Snail expression was abrogated by the addition of the ROS-quenching reagent, NAC. NAC inhibited phosphorylation of Erk, its binding to the Snail promoter, and phosphorylation of GSK-3β by blocking intracellular ROS accumulation, leading to reduction of Snail expression. Based on these findings, it is likely that overproduction of ROS could be a plausible link between *H. pylori* and activation of Erk and inactivation of GSK-3β pathways.

Overexpression of Snail has been associated with invasion, metastasis and poor prognosis, particularly in gastric cancer [12,39]. Once Snail is inactivated, invasive and metastatic capability of cancer cells could be diminished [40,41]. Since the ROS scavenger NAC abolished *H. pylori*-induced Snail expression, ROS-quenching agents or regimen capable of potentiating body's antioxidant capacity could be utilized in the management of gastric cancer caused by *H. pylori* infection.

In summary, our study reveals that *H. pylori* infection overproduces ROS and subsequently upregulates expression of Snail via multiple mechanisms. These include the increase in Snail transcription, the prevention of Snail protein degradation, and the enhancement of Snail nuclear localization, which partly involves activation of Erk and inactivation of GSK-3β as schematically proposed in Figure 6.

AUTHORS' CONTRIBUTIONS

HKCN designed, performed experiments, analyzed data, and wrote the manuscript. HGL, JYP, ZXC, HNL, HJH, WKK performed the experiments. YNC, DHK, HKN participated in study design and discussion. YJS supervised the whole study and edited the manuscript. All authors read and approved the final manuscript.

ACKNOWLEDGMENTS

This work was supported by the Global Core Research Center (GCRC) grant (No. 2011-0030001) from the National Research Foundation (NRF), Republic of Korea.

REFERENCES

1. Polk DB, Peek RM, Jr. *Helicobacter pylori*: Gastric cancer and beyond. Nat Rev Cancer 2010;10:403–414.
2. Amieva MR, El-Omar EM. Host-bacterial interactions in *Helicobacter pylori* infection. Gastroenterology 2008;134: 306–323.
3. Peek RM, Jr., Crabtree JE. *Helicobacter* infection and gastric neoplasia. J Pathol 2006;208:233–248.
4. Correa P. Human gastric carcinogenesis: A multistep and multifactorial process—First American Cancer Society Award Lecture on Cancer Epidemiology and Prevention. Cancer Res 1992;52:6735–6740.
5. Yin Y, Grabowska AM, Clarke PA, et al. *Helicobacter pylori* potentiates epithelial: Mesenchymal transition in gastric cancer: Links to soluble HB-EGF, gastrin, and matrix metalloproteinase-7. Gut 2010;59:1037–1045.
6. Baud J, Varon C, Chabas S, Chambonnier L, Darfeuille F, Staedel C. *Helicobacter pylori* initiates a mesenchymal transition through ZEB1 in gastric epithelial cells. PLoS ONE 2013;8:e60315.
7. Barrallo-Gimeno A, Nieto MA. The Snail genes as inducers of cell movement and survival: Implications in development and cancer. Development 2005;132:3151–3161.
8. Vega S, Morales AV, Ocana OH, Valdes F, Fabregat I, Nieto MA. Snail blocks the cell cycle and confers resistance to cell death. Genes Dev 2004;18:1131–1143.
9. Shin NR, Jeong EH, Choi CI, et al. Overexpression of Snail is associated with lymph node metastasis and poor prognosis in patients with gastric cancer. BMC Cancer 2012;12:521.
10. Park SA, Na HK, Kim EH, Cha YN, Surh YJ. 4-hydroxyestradiol induces anchorage-independent growth of human mammary epithelial cells via activation of IkappaB kinase: Potential role of reactive oxygen species. Cancer Res 2009;69:2416–2424.
11. Ikenouchi J, Matsuda M, Furuse M, Tsukita S. Regulation of tight junctions during the epithelium-mesenchyme transition: Direct repression of the gene expression of claudins/occludin by Snail. J Cell Sci 2003;116:1959–1967.
12. Kudo-Saito C, Shirako H, Takeuchi T, Kawakami Y. Cancer metastasis is accelerated through immunosuppression during Snail-induced EMT of cancer cells. Cancer Cell 2009;15:195–206.
13. Saito Y, Murata-Kamiya N, Hirayama T, Ohba Y, Hatakeyama M. Conversion of *Helicobacter pylori* CagA from senescence inducer to oncogenic driver through polarity-dependent regulation of p21. J Exp Med 2010;207:2157–2174.
14. Bessede E, Staedel C, Acuna Amador LA, et al. *Helicobacter pylori* generates cells with cancer stem cell properties via epithelial-mesenchymal transition-like changes. Oncogene 2014;33:4123–4131.
15. Lee DG, Kim HS, Lee YS, et al. *Helicobacter pylori* CagA promotes Snail-mediated epithelial-mesenchymal transition by reducing GSK-3 activity. Nat Commun 2014;5:4423.
16. Wang XJ, Yang J, Cang H, Zou YQ, Yi J. Gene expression alteration during redox-dependent enhancement of arsenic cytotoxicity by emodin in HeLa cells. Cell Res 2005;15: 511–522.
17. Ziech D, Franco R, Pappa A, Panayiotidis MI. Reactive oxygen species (ROS)-induced genetic and epigenetic alterations in human carcinogenesis. Mutat Res 2011;711:167–173.
18. Arora S, Bhardwaj A, Singh S, et al. An undesired effect of chemotherapy: Gemcitabine promotes pancreatic cancer cell invasiveness through ROS-dependent, NF-kappaB-, and HIF-1alpha-mediated upregulation of CX CR4. J Biol Chem 2013;288:21197–21207.
19. Lin X, Zheng W, Liu J, et al. Oxidative stress in malignant melanoma enhances tumor necrosis factor-alpha secretion of tumor-associated macrophages that promote cancer cell invasion. Antioxid Redox Signal 2013;19:1337–1355.
20. Calvino-Fernandez M, Benito-Martinez S, Parra-Cid T. Oxidative stress by *Helicobacter pylori* causes apoptosis through mitochondrial pathway in gastric epithelial cells. Apoptosis 2008;13:1267–1280.
21. Handa O, Naito Y, Yoshikawa T. *Helicobacter pylori*: A ROS-inducing bacterial species in the stomach. Inflamm Res 2010;59:997–1003.
22. Wu HW, Li HF, Wu XY, Zhao J, Guo J. Reactive oxygen species mediate ERK activation through different Raf-1-dependent signaling pathways following cerebral ischemia. Neurosci Lett 2008;432:83–87.
23. Santamaria PG, Nebreda AR. Deconstructing ERK signaling in tumorigenesis. Mol Cell 2010;38:3–5.
24. Xie L, Law BK, Chytil AM, Brown KA, Aakre ME, Moses HL. Activation of the Erk pathway is required for TGF-beta1-induced EMT in vitro. Neoplasia 2004;6:603–610.

25. Zhang K, Corsa CA, Ponik SM, et al. The collagen receptor discoidin domain receptor 2 stabilizes SNAIL1 to facilitate breast cancer metastasis. Nat Cell Biol 2013;15:677–687.
26. Barbera MJ, Puig I, Dominguez D, et al. Regulation of Snail transcription during epithelial to mesenchymal transition of tumor cells. Oncogene 2004;23:7345–7354.
27. Doble BW, Woodgett JR. GSK-3: Tricks of the trade for a multi-tasking kinase. J Cell Sci 2003;116:1175–1186.
28. Fang X, Yu SX, Lu Y, Bast RC, Jr., Woodgett JR, Mills GB. Phosphorylation and inactivation of glycogen synthase kinase 3 by protein kinase A. Proc Natl Acad Sci USA 2000;97: 11960–11965.
29. Ryu YK, Lee YS, Lee GH, Song KS, Kim YS, Moon EY. Regulation of glycogen synthase kinase-3 by thymosin beta-4 is associated with gastric cancer cell migration. Int J Cancer 2012;131:2067–2077.
30. Yang J, Duh EJ, Caldwell RB, Behzadian MA. Antipermeability function of PEDF involves blockade of the MAP kinase/GSK/ beta-catenin signaling pathway and uPAR expression. Invest Ophthalmol Vis Sci 2010;51:3273–3280.
31. Zhou BP, Deng J, Xia W, et al. Dual regulation of Snail by GSK-3beta-mediated phosphorylation in control of epithelial-mesenchymal transition. Nat Cell Biol 2004;6:931–940.
32. Dominguez D, Montserrat-Sentis B, Virgos-Soler A, et al. Phosphorylation regulates the subcellular location and activity of the snail transcriptional repressor. Mol Cell Biol 2003;23: 5078–5089.
33. Wu Y, Deng J, Rychahou PG, Qiu S, Evers BM, Zhou BP. Stabilization of snail by NF-kappaB is required for inflammation-induced cell migration and invasion. Cancer Cell 2009;15:416–428.
34. Nagarajan D, Melo T, Deng Z, Almeida C, Zhao W. ERK/GSK3beta/Snail signaling mediates radiation-induced alveolar epithelial-to-mesenchymal transition. Free Radic Biol Med 2012;52:983–992.
35. Pon YL, Zhou HY, Cheung AN, Ngan HY, Wong AS. P70 S6 kinase promotes epithelial to mesenchymal transition through snail induction in ovarian cancer cells. Cancer Res 2008;68:6524–6532.
36. Yang Z, Rayala S, Nguyen D, Vadlamudi RK, Chen S, Kumar R. Pak1 phosphorylation of snail, a master regulator of epithelial-to-mesenchyme transition, modulates snail's subcellular localization and functions. Cancer Res 2005;65: 3179–3184.
37. Yook JI, Li XY, Ota I, et al. A Wnt-Axin2-GSK3beta cascade regulates Snail1 activity in breast cancer cells. Nat Cell Biol 2006;8:1398–1406.
38. Machado AM, Desler C, Boggild S, et al. *Helicobacter pylori* infection affects mitochondrial function and DNA repair, thus, mediating genetic instability in gastric cells. Mech Ageing Dev 2013;134:460–466.
39. Yuan H, Kajiyama H, Ito S, et al. ALX1 induces snail expression to promote epithelial-to-mesenchymal transition and invasion of ovarian cancer cells. Cancer Res 2013;73: 1581–1590.
40. Guo HM, Zhang XQ, Xu CH, Zou XP. Inhibition of invasion and metastasis of gastric cancer cells through snail targeting artificial microRNA interference. Asian Pac J Cancer Prev 2011;12:3433–3438.
41. Ferrari-Amorotti G, Fragliasso V, Esteki R, et al. Inhibiting interactions of lysine demethylase LSD1 with snail/slug blocks cancer cell invasion. Cancer Res 2013;73:235–245.